

Article

Mesoxalate-Bridged Heptanuclear Copper(II) Complexes: Structure and Magnetic Properties †

Beatriz Gil-Hernández ^{1,2}, Simon Millan ³, Irina Gruber ³, Christoph Janiak ³ , Carlos J. Gómez-García ⁴ 
and Joaquín Sanchiz ^{1,2,*} 

¹ Departamento de Química, Facultad de Ciencias, Universidad de La Laguna, 38206 La Laguna, Santa Cruz de Tenerife, Spain; beagher@ull.edu.es

² Instituto Universitario de Materiales y Nanotecnología (IMN), Universidad de La Laguna, 38206 La Laguna, Santa Cruz de Tenerife, Spain

³ Institut für Anorganische Chemie und Strukturchemie, Heinrich-Heine-Universität, 40204 Düsseldorf, Germany; janiak@uni-duesseldorf.de (C.J.)

⁴ Departamento de Química Inorgánica, Universidad de Valencia, Dr Moliner 50, 46100 Burjassot, Valencia, Spain; carlos.gomez@uv.es

* Correspondence: jsanchiz@ull.edu.es; Tel.: +34-922845425

† This work is dedicated to Prof. Miguel Julve and Prof. Francesc Lloret. With this work, we wish to contribute to the tribute and international recognition of our colleagues Paco and Miguel. We are deeply saddened by Miguel's recent passing, and we cannot let this occasion pass without paying our small tribute to him and his work. We have been fortunate to know both Paco and Miguel for a long time, and we have witnessed their active participation in the development of the field known as molecular magnetism. Thanks to the brilliance and creativity of their work, they have advanced knowledge in this field and inspired many researchers who have joined their cause. Now, all of us express our gratitude by offering them this recognition. Thank you both for sharing your wisdom and motivation with us.

Abstract: Two new compounds, $(\text{NH}_4)_4[\text{Cu}_7(\text{Hmesox})_6(\text{H}_2\text{O})_8]\cdot 10\text{H}_2\text{O}$ (**1**) and $[\text{Ru}(\text{bpy})_3]_4[\text{Cu}_7(\text{Hmesox})_6\text{Cl}_2]\text{Cl}_2\cdot 2\text{CH}_3\text{CN}\cdot 12\text{H}_2\text{O}$ (**2**), were prepared and their structures were solved by single-crystal X-ray diffraction (mesoxalic acid = dihydroxypropanedioic acid, H_4mesox). The triply deprotonated mesoxalate anion acts as a chelating and bridging ligand with its carboxylate and alkoxide groups, forming the anionic heptanuclear copper(II) clusters $[\text{Cu}_7(\text{Hmesox})_6(\text{H}_2\text{O})_8]^{4-}$ and $[\text{Cu}_7(\text{Hmesox})_6\text{Cl}_2]^{6-}$ in **1** and **2**, respectively. Variable temperature magnetic studies revealed anti-ferromagnetic interactions in **1** and the coexistence of ferro and antiferromagnetic interactions in **2**. The $[\text{Ru}(\text{bpy})_3]^{2+}$ cations provided luminescent properties to compound **2**.

Keywords: heptanuclear Cu(II) complexes; mesoxalate; magnetic properties; crystal structure; luminescence



Citation: Gil-Hernández, B.; Millan, S.; Gruber, I.; Janiak, C.; Gómez-García, C.J.; Sanchiz, J. Mesoxalate-Bridged Heptanuclear Copper(II) Complexes: Structure and Magnetic Properties. *Magnetochemistry* **2024**, *10*, 93. <https://doi.org/10.3390/magnetochemistry10120093>

Academic Editor: Ming-Liang Tong

Received: 29 October 2024

Revised: 14 November 2024

Accepted: 19 November 2024

Published: 22 November 2024



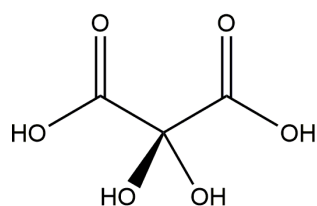
Copyright: © 2024 by the authors. Licensee MDPI, Basel, Switzerland. This article is an open access article distributed under the terms and conditions of the Creative Commons Attribution (CC BY) license (<https://creativecommons.org/licenses/by/4.0/>).

1. Introduction

The field formerly known as molecular magnetism underwent significant development, both experimentally and theoretically, in the 1980s, and since then, there has been a continuous stream of research in this area, yielding a plethora of compounds with intriguing magnetic properties and behaviours. Two key figures in the advancement of this field have undoubtedly been Professors Miguel Julve and Francesc Lloret from the University of Valencia. Sadly, Professor Julve passed away this year, and Professor Lloret will retire (although not completely) during 2024. Thanks to their pioneering work and the efforts of an entire community of researchers, numerous advancements have occurred in this field. The University of La Laguna has also contributed to the growth of this field, and we take this opportunity to pay tribute to our colleagues.

Many of the studies conducted by these researchers, especially in the early stages, focused on the investigation of magneto-structural correlations with ligands containing carboxylate and hydroxyl groups [1–5]. To a large extent, these studies established the factors influencing the intensity and nature of the magnetic interaction between paramagnetic

ions, particularly Cu^{II} ions, bridged by those ligands. At the University of La Laguna, some researchers have collaborated over the years with Professors Julve and Lloret, studying the chemistry and properties of malonate as a ligand [6], and more recently utilizing the mesoxalate ligand (the conjugated base of 2,2-dihydroxypropanedioic acid, Scheme 1), which contains not only two carboxylate groups but also two alcohol groups, mediating magnetic interaction not only through the carboxylate but also through at least one alkoxide group. Combined with Cu^{II}, this ligand yields trinuclear [Cu₃(Hmesox)₃]^{3−} species that can be used as a ferromagnetically or antiferromagnetically coupled secondary building units [7,8]. Combining this trinuclear unit with Cu^{II} or other 3d metallic ions such as Mn^{II}, Co^{II}, Ni^{II} or some Ln^{III} ions, we have prepared chiral three-dimensional MOFs, some of them exhibiting long-range magnetic ordering or proton conduction [9,10].



Scheme 1. Mesoxalic acid, H₄mesox.

However, up to now, we have not studied the formation of species of lower dimensionality, such as discrete high-nuclearity molecules, and we scarcely explored the preparation of compounds that combine other properties apart from magnetism and proton conduction. In this work, we describe two new compounds which are the first examples of mesoxalate-bridged heptanuclear copper(II) clusters (NH₄)₄[Cu₇(Hmesox)₆(H₂O)₈·10H₂O (**1**) and [Ru(bpy)₃]₄[Cu₇(Hmesox)₆Cl₂][Cl₂·2 CH₃CN·12H₂O (**2**). Heptanuclear copper(II) clusters is a topic of current interest in molecular magnetism, and compounds exhibiting ferromagnetic and antiferromagnetic interactions and less frequent magnetic phenomena, such as antisymmetric exchange interactions, have been recently prepared and studied [11,12]. Compounds **1** and **2** are both built from the [Cu₃(Hmesox)₃]^{3−} secondary building unit and exhibit different magnetic properties due to small structural differences. Moreover, compound **2** incorporates a luminescent counterion and displays additional luminescent properties.

2. Materials and Methods

2.1. Materials

Copper (II) acetate hydrate, basic copper (II) carbonate, mesoxalic acid disodium salt, cation exchange resin Amberlite IR-120, 20% aqueous ammonia, acetonitrile, methanol and diethyl ether were purchased from commercial sources and used as received. Tris(bipyridine)ruthenium(II) chloride hexahydrate, [Ru(bpy)₃Cl₂·6H₂O], was obtained by the method reported by Bromhead and Young [13].

2.2. Characterization

Elemental CHN analysis was performed with a Perkin-Elmer CHN 2400 (Perkin-Elmer, Waltham, MA, USA). IR spectra (400–4000 cm^{−1}) were recorded on a Thermo-Nicolet avatar 360 FT-IR spectrometer with the sample prepared as KBr disks. X-ray powder diffraction patterns on the polycrystalline samples of **1–2** (Supplementary Material: Figures S1 and S2, respectively) were collected with a PANalytical X'pert X-ray diffractometer (Cu K_{α,1} radiation = 1.54184 Å) at room temperature.

Magnetic measurements were performed in a Quantum Design MPMS XL-5 magnetometer with an applied magnetic field of 1 T (in the temperature range 15–300 K) and with an applied magnetic field of 100 mT (in the range 2–15 K). The susceptibility data were corrected for the sample holder, measured under the same conditions and for the diamagnetic contribution, evaluated using Pascal's constants [14].

Emission spectra were obtained by exciting the samples with light from a 350 W Xe arc lamp passed through a 0.25 m double monochromator (Spex 1680, Spex Industries, Metuchen, NJ, USA). Fluorescence was detected using a 0.25 m monochromator (Spex 1681) with a photomultiplier (Hamamatsu R928, Hamamatsu Photonics, Hamamatsu, Japan). The luminescence decay was measured using an optical parametric oscillator laser (EKSPLA, Vilnius, Lithuania), with excitation at 480 nm and detection at 600 nm. The signal acquired with the photomultiplier was registered in an oscilloscope (Tektronix 2430, Tectronix Inc., Beaverton, OR, USA) controlled by a computer.

2.3. Synthesis of $(\text{NH}_4)_4[\text{Cu}_7(\text{Hmesox})_6(\text{H}_2\text{O})_8]\cdot 10\text{H}_2\text{O}$ (**1**)

Solid disodium mesoxalate (180 mg, 1 mmol) was added to a suspension of the cation exchange resin Amberlite IR-120 (1.5 g in 5 mL of water) in order to obtain a mesoxalic acid solution (H_4mesox). This suspension was filtered through a Büchner funnel, and the filtrate was collected in a beaker. To this solution, 20% aqueous ammonia (115 μL , 1.5 mmol) was added, followed by the addition of 8 mL of a copper(II) acetate aqueous solution (200 mg, 1.1 mmol) under continuous stirring. Prismatic blue single-crystals of **1**, obtained after one week, were filtered and washed with water and air-dried at room-temperature. Yield: 148 mg (54%). IR spectra main peaks (cm^{-1}): 3447, 3207, 1654 (s,b), 1400 (s), 1346 (s), 1084 (s), 865 (w), 819 (w), 668 (w), 485 (w). Anal. Calc. for air-dried $\text{C}_{18}\text{H}_{50}\text{Cu}_7\text{N}_4\text{O}_{50}$ (four crystallization molecules were lost respect to the single crystal): C, 13.79; H, 3.22; N, 3.57%. Found: C, 13.83; H, 3.22; N, 3.45%.

2.4. Synthesis of $[\text{Ru}(\text{bpy})_3]_4[\text{Cu}_7(\text{Hmesox})_6\text{Cl}_2]\text{Cl}_2\cdot 2\text{CH}_3\text{CN}\cdot 12\text{H}_2\text{O}$ (**2**)

A mesoxalic acid solution (0.5 mmol, 5 mL) was obtained as in the synthesis of **1**. To this solution, solid basic copper(II) carbonate (55 mg, 0.25 mmol) was added, and the suspension was stirred and heated at 40 °C for 20 min. The resultant solution was filtered, diluted to 10 mL, and solid copper(II) acetate (50 mg, 0.25 mmol) was added under stirring. Finally, 4 mL of a 50:50 water/acetonitrile solution of $[\text{Ru}(\text{bpy})_3]\text{Cl}_2$ (250 mg, 0.33 mmol) was added. The solution was allowed to stand at room-temperature, and prismatic dark-red single-crystals of **2** were obtained within 5 days. Yield 95 mg, 29%. IR (cm^{-1}): 3428 (b), 1647 (s,b), 1420 (s), 1336 (s), 1102 (s), 865 (w), 822 (w), 774 (w), 659 (w). Anal. Calc. for air-dried $\text{C}_{142}\text{H}_{132}\text{Cl}_4\text{Cu}_7\text{N}_{26}\text{O}_{48}\text{Ru}_4$: C, 43.02; H, 3.36; N, 9.19%. Found: C, 42.95; H, 3.33; N, 9.13%.

2.5. X-Ray Data Collection and Structure Refinement

Suitable single-crystals of **1** and **2** were selected in the microscope, covered with protective oil and mounted on a 50 μm loop. Data collection for compound **1** was performed on a Bruker Kappa APEX2 CCD X-ray diffractometer (Bruker AXS Inc., Madison, WI, USA) with a microfocus tube, Cu-K α radiation ($\lambda = 1.5418 \text{ \AA}$) and a multilayer mirror system. The data were collected using ω scans, with the collection performed using APEX2 [15], cell refinement carried out with SMART, data reduction performed using SAINT [15] and experimental absorption correction performed with SADABS [16]. The structure was solved by direct methods (SHELXS-2016), refinement was achieved by full-matrix least squares on F² using the SHELXL-2016 program suite [17], and the graphical user interface (GUI) ShelXle was used [18]. Crystal data and details on the structure refinement are given in Table 1 and Appendix A. Hydrogen atoms on the mesoxalate hydroxyl groups were positioned geometrically (O-H = 0.83 Å) and refined using a riding model (AFIX 83) with U_{iso}(H) = 1.5 U_{eq}(O). H atoms on the oxygen atoms of both coordination and crystallization water molecules could not be located. H atoms of the ammonium cations could not be located either. Nevertheless, all of them were included in the UNIT card for the calculation of the sum formula. The data collection for compound **2** was performed on a Bruker–Nonius Kappa CCD diffractometer equipped with graphite-monochromated Mo-K α ($\lambda = 0.71073 \text{ \AA}$) using COLLECT [19]. Data reduction was carried out with HKL DENZO and SCALEPACK [20], and experimental absorption correction was applied using

SADABS [16]. The structure was solved by direct methods using SHELXS97 [21] and refinement was achieved by full-matrix least squares on F2 using the SHELXL97 program suite [21]. Crystal data and details on the structure refinement are given in Table 1 and Appendix A. The θ range is relatively low because the crystals obtained were very small and did not diffract well beyond a certain threshold. Despite several attempts to obtain higher-quality crystals, these efforts were unsuccessful. The hydrogen atoms for aromatic C–H and methyl groups were positioned geometrically (C–H = 0.94 Å for aromatic C–H and C–H = 0.97 Å for CH₃) and refined using a riding model (AFIX 43 for aromatic C–H, rotating group refinement AFIX 137 for CH₃), with Uiso(H) = 1.2Ueq (C–H) and Uiso(H) = 1.5 Ueq (CH₃), respectively. The H atoms of the hydroxyl central mesoxalate groups could not be found or refined. The H atoms of the oxygen atoms of crystallization water could not be located, but they were included in the UNIT card for the calculation of the sum formula. The carbon atoms of the bipyridine ligands of Ru2 were refined only isotropically in view of the low number of reflections and the reflection/parameter ratio. The pyridyl groups of Ru1 were refined as a regular hexagon (AFIX 66/65) to lower the number of independent parameters for a still reasonable reflection/parameter ratio.

Table 1. Summary of crystallographic data for complexes 1 and 2.

Compound	1	2
Empirical formula	C ₁₈ H ₅₈ Cu ₇ N ₄ O ₅₄	C ₁₄₂ H ₁₃₂ Cl ₄ Cu ₇ N ₂₆ O ₄₈ Ru ₄
M (g mol ^{−1})	1639.46	3955.55
Temperature (K)	296	296
λ (Å)	1.54178	0.71073
Crystal system	Monoclinic	Monoclinic
Space group	<i>P</i> 2 ₁ / <i>c</i>	<i>P</i> 2 ₁ / <i>c</i>
<i>a</i> (Å)	10.1046(5)	13.6168(2)
<i>b</i> (Å)	32.7505(16)	22.0785(3)
<i>c</i> (Å)	7.8273(4)	24.6442(5)
β (°)	104.742(2)	90.395(1)
<i>V</i> (Å ³)	2505.0(2)	7408.8(2)
<i>Z</i>	2	2
<i>D</i> _{calc} (g cm ^{−3})	2.174	1.762
μ (mm ^{−1})	4.56	1.55
Theta range (°)	4.5–67.2	4.4–21.2
Unique reflections	26,616	27,089
<i>R</i> _{int}	0.043	0.029
GOF on <i>F</i> ²	1.07	1.05
<i>R</i> ₁ [<i>I</i> > 2 σ (<i>I</i>)] ^a	0.0663	0.044
<i>wR</i> ₂ [<i>I</i> > 2 σ (<i>I</i>)] ^b	0.193	0.110
CCDC number	1909005	1909004

$$^a R_1 = [\sum(|F_o| - |F_c|) / \sum |F_o|]; ^b wR_2 = [\sum[w(F_o^2 - F_c^2)^2] / \sum[w(F_o^2)^2]]^{1/2}.$$

3. Results and Discussion

3.1. Crystal Structures of Compounds 1 and 2

3.1.1. Crystal Structure of (NH₄)₄[Cu₇(Hmesox)₆(H₂O)₈]·10 H₂O (1)

Compound 1 crystallizes in the monoclinic centrosymmetric space group *P*2₁/*c*. The asymmetric unit contains three mesoxalate ligands, four copper atoms, two counterbalancing ammonium cations, four coordination water molecules and five crystallization

water molecules. The structure of **1** consists of ammonium cations, crystallization water molecules and an anionic centrosymmetric heptanuclear copper(II) cluster, which can be seen as two trinuclear copper(II)-mesoxalate entities, $[\text{Cu}_3(\text{Hmesox})_3(\text{H}_2\text{O})_3]^{3-}$, linked by a central copper(II) ion (Cu1) (Figure 1).

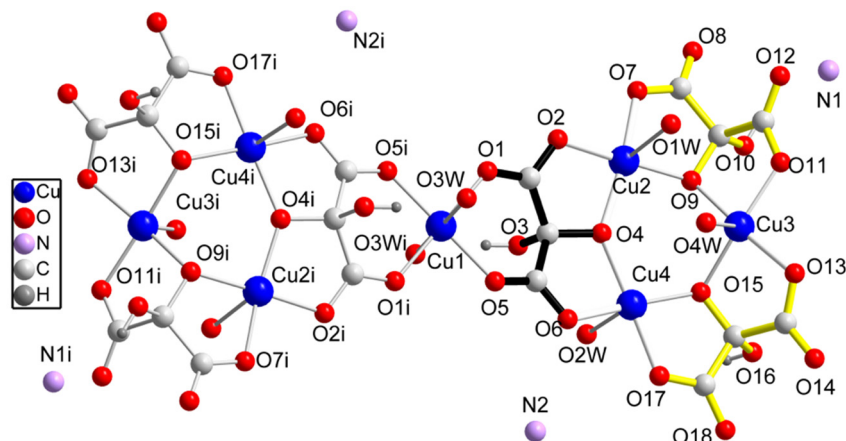


Figure 1. Structure of the centrosymmetric $[\text{Cu}_7(\text{Hmesox})_6(\text{H}_2\text{O})_8]^{4-}$ heptanuclear cluster in **1** with the nitrogen atoms of the ammonium counter ions. Central mesoxalate highlighted in black, peripheral mesoxalates highlighted in yellow. C and H atom labels are omitted for clarity. Symmetry code: (i) $1 - x, 1 - y, -z$.

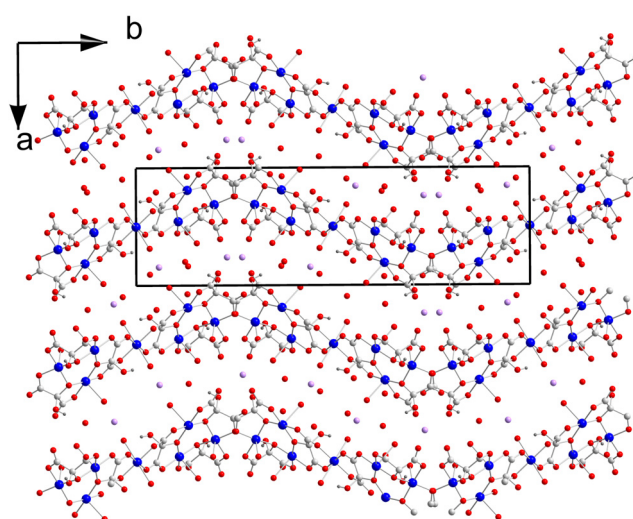
All the mesoxalate ligands are triply deprotonated, $\text{HC}_3\text{O}_6^{3-}$ ($\text{Hmesox})^{3-}$ keeping only one of their four protons and acting as coordinating and bridging ligand among the copper atoms. The two peripheral mesoxalates (shown in yellow in Figure 1) act as blocking, but also as bridging ligands between Cu4–Cu3 and Cu3–Cu2 through μ -alkoxido oxygens (O15 and O9, respectively). The central mesoxalate (shown in black in Figure 1) acts as μ_3 -bridging ligand connecting Cu4–Cu2–Cu1 centres. Cu2 and Cu4 are connected through a μ -alkoxido-oxygen, whereas Cu2–Cu1 and Cu4–Cu1 connections are performed with two *anti-anti* carboxylate groups. One of the central hydroxyl groups of all the mesoxalate ligands remains protonated and uncoordinated. The mesoxalate–alkoxido and carboxylato oxygens occupy the basal positions of the Cu2, Cu3 and Cu4 atoms and form five-membered chelate rings with the skeleton of the mesoxalate ligand. These three copper ions display a square-pyramidal coordination geometry with τ parameters of 0.15 for Cu2, 0.12 for Cu3 and 0.03 for Cu4 [22]. The basal Cu–O distances for all these Cu^{II} ions lie in the range 1.9298(1)–1.9525(1) Å (Table 2). The apical positions are occupied by a water molecule in the three Cu ions with longer distances ranging from 2.4198(1) to 2.4717(1) Å (Table 2). All these bond distances are in agreement with other copper(II)–mesoxalate complexes [23]. Cu2, Cu3 and Cu4 atoms assemble with the three mesoxalate ligands into trinuclear $[\text{Cu}_3(\text{Hmesox})_3(\text{H}_2\text{O})_3]^{3-}$ entities, which appear in other Cu(II)–mesoxalate compounds [23,24]. The trinuclear unit exhibits a distorted isosceles triangular structure with two small [$\text{Cu4-O15-Cu3} = 119.218(2)^\circ$ and $\text{Cu3-O9-Cu2} = 118.779(2)^\circ$] and one long [$\text{Cu4-O4-Cu2} = 139.387(2)^\circ$] Cu–O–Cu bridging angles (Table 2).

The Cu1 atom sits on an inversion centre and bridges the two trinuclear entities forming the heptanuclear copper(II)-mesoxalate cluster. The mesoxalate ligands around this copper(II) ion form two six-membered chelate rings. The 4 + 2 Jahn-Teller distorted-octahedral coordination environment of Cu1 is completed with two water molecules filling the axial positions at distances of 2.4275(1) Å. The heptanuclear cluster has a net charge of -4 , which is balanced by 4 ammonium cations.

The supramolecular packing (Figure 2) of these heptanuclear copper (II) clusters takes place through hydrogen bonding among the ammonium cations and the coordinated water molecules that stabilize the three-dimensional structure (Table 3).

Table 2. Selected bond lengths (Å) and angles (°) for compound 1.

Atoms	Distance (Å)	Atoms	Distance (Å)	Atoms	Angle (°)
Cu1–O5	1.940(5)	Cu3–O9	1.935(4)	Cu4–O4–Cu2	139.4(2)
Cu1–O1	1.952(5)	Cu3–O15	1.948(4)	Cu2–O9–Cu3	118.8(2)
Cu1–O3W	2.427(5)	Cu3–O4W	2.437(5)	Cu3–O15–Cu4	119.2(2)
Cu2–O9	1.926(4)	Cu4–O4	1.953(4)		
Cu2–O2	1.933(5)	Cu4–O17	1.935(5)		
Cu2–O7	1.939(5)	Cu4–O6	1.945(4)		
Cu2–O4	1.957(4)	Cu4–O15	1.949(4)		
Cu3–O11	1.930(4)	Cu1–Cu2	5.514(6)		
Cu3–O13	1.930(4)	Cu1–Cu4	5.528(6)		

**Figure 2.** Supramolecular packing of the heptanuclear copper(II) clusters in compound 1 (same colour code as in Figure 1).**Table 3.** Short intermolecular contacts involved in hydrogen bonding (Å) for compound 1 (the H atoms of the water and ammonium molecules could not be located or refined).

D–H...A	D...A	D–H...A	D...A	D–H...A	D...A
O1W...O9W	2.835	O2W...N2 ⁱⁱⁱ	2.779	O12...N1 ^{vi}	2.866
O2...N2	2.803	O7...O3W ^{iv}	2.723	O18...N1 ⁱⁱⁱ	2.836
O2W...O5W ⁱⁱ	2.554	O12...N1 ^v	2.818	O18...N1 ^{vii}	2.865

ii = $-1 + x, y, -1 + z$; iii = $-1 + x, y, z$; iv = $1 - x, -y, -z$; v = $x, y, -1 + z$; vi = $x, 0.5 - y, -0.5 + z$; vii = $-1 + x, 0.5 - y, -0.5 + z$.

3.1.2. Crystal Structure of $[\text{Ru}(\text{bpy})_3]_4[\text{Cu}_7(\text{Hmesox})_6\text{Cl}_2]\text{Cl}_2 \cdot 2\text{CH}_3\text{CN} \cdot 12\text{H}_2\text{O}$ (2)

Compound 2 also crystallizes in the monoclinic centrosymmetric space group $P2_1/c$. The asymmetric unit contains three mesoxalate ligands, four copper atoms, two chloride anions, two $[\text{Ru}(\text{bpy})_3]^{2+}$ cations, one CH_3CN and five crystallization water molecules (Figure 3). The centrosymmetric heptanuclear copper(II) cluster is very similar to that of 1: it consists of two $[\text{Cu}_3(\text{Hmesox})_3\text{Cl}]^{4-}$ trinuclear units bridged by a central copper(II) ion. In the asymmetric unit, two of the mesoxalate ligands (depicted in yellow in Figure 3) act as chelating and bridging agents between two copper(II) ions (Cu2–Cu3 and Cu3–Cu4), whereas the third one (shown in black in Figure 3) acts as a μ_3 -bridge between Cu1–Cu2–Cu4.

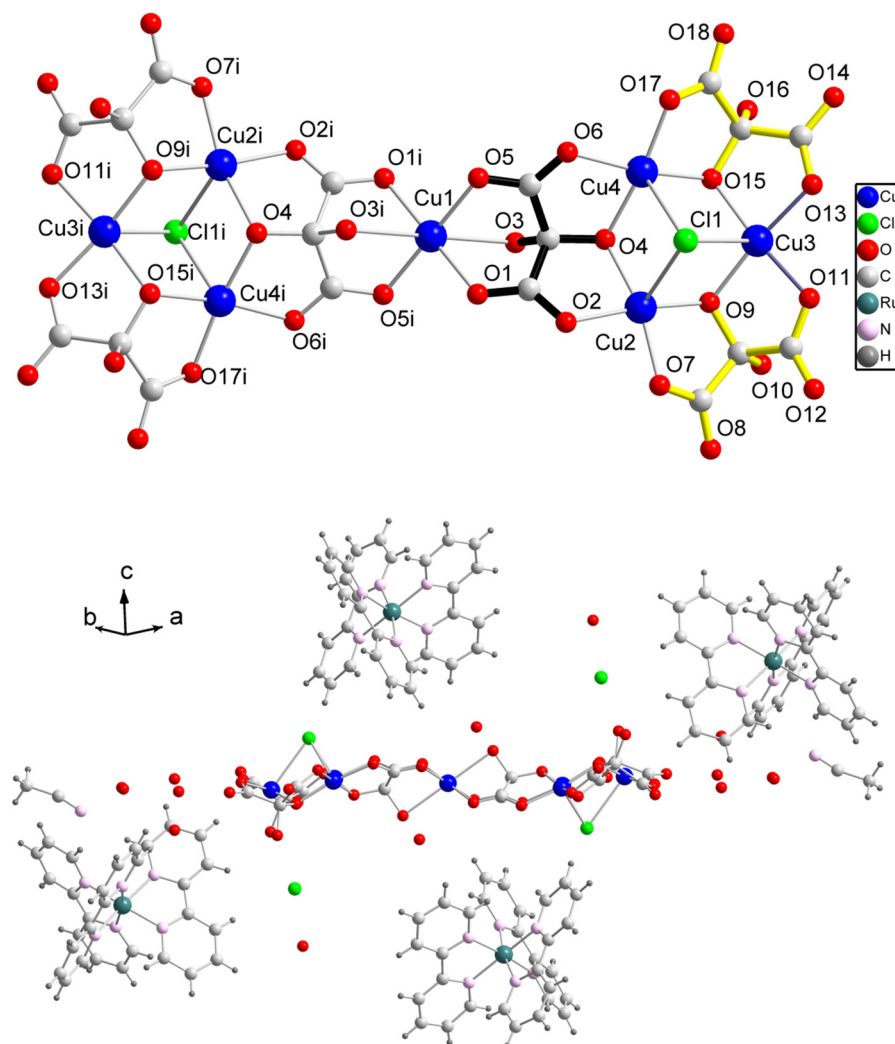


Figure 3. (top) Molecular structure of the heptanuclear cluster in **2**, with the labelling scheme of the main atoms. Symmetry code: (i) $1 - x, 1 - y, -z$ (bottom). View of one heptanuclear cluster surrounded by four $[\text{Ru}(\text{bpy})_3]^{2+}$ cations, crystallization water and CH_3CN molecules.

The bridging modes and the protonation degree of the mesoxalate ligands are analogous to those observed in **1**. The copper(II) ions in the triangular units, Cu2, Cu3 and Cu4, display very slightly distorted square-pyramidal environments with τ parameters of 0.15, 0.02 and 0.06, respectively [22]. They all present four mesoxalate oxygens in the basal positions (two alkoxido and two carboxylate-oxygens from two different mesoxalate ligands) and a $\mu_3\text{-Cl}^-$ in the apical position. The basal Cu–O and Cu–Cl bond distances are in the range 1.903(4)–1.981(4) Å and 2.643(2)–2.821(2) Å, respectively (Table 4). These values are similar to those observed in other related compounds [23]. The $\mu_3\text{-Cl}^-$ bridge at the apical position is one of the main differences between the heptanuclear clusters of **1** and **2** and results in much smaller Cu–O–Cu bridging angles, which have capital importance in the magnetic behaviour. The other main difference is the elongated and trigonally-distorted octahedral environment of Cu1, resulting from the coordination of four mesoxalate carboxylate-oxygens (from two mesoxalate ligands, as in **1**) and two mesoxalate hydroxyl groups (in contrast to the two water molecules observed in **1**). The basal Cu1–O1 and Cu1–O5 distances are 1.954(4) Å and 1.984(4) Å, respectively, and the long axial one is Cu1–O3 2.459(4) Å.

Table 4. Selected bond lengths (Å) and angles (°) for compound 2.

Atoms	Distance (Å)	Atoms	Distance (Å)	Atoms	Angle (°)
Cu1–O5	1.954(4)	Cu4–Cl1	2.728(2)	Cu2–Cl1–Cu4	74.46(5)
Cu1–O1	1.984(4)	Ru1–N4	2.056(3)	Cu2–O9–Cu3	113.18(19)
Cu2–O7	1.925(5)	Ru1–N6	2.059(3)	Cu4–O4–Cu2	111.39(18)
Cu2–O9	1.932(4)	Ru1–N1	2.063(3)	Cu4–O4–Cu2	111.39(18)
Cu1–O3	2.459(4)	Ru1–N5	2.067(2)	Cu4–O15–Cu3	112.34(19)
Cu2–O2	1.966(4)	Ru1–N2	2.070(3)	Cu4–O15–Cu3	112.34(19)
Cu2–O4	1.981(4)	Ru1–N3	2.070(3)		
Cu2–Cl1	2.643(2)	Ru2–N12	2.053(5)		
Cu3–O13	1.914(5)	Ru2–N11	2.055(5)		
Cu3–O11	1.914(5)	Ru2–N8	2.055(5)		
Cu3–O15	1.946(4)	Ru2–N9	2.056(5)		
Cu3–O9	1.947(4)	Ru2–N7	2.062(5)		
Cu3–Cl1	2.821(2)	Ru2–N10	2.067(5)		
Cu4–O17	1.903(4)	Cu1–Cu2	5.3078(7)		
Cu4–O15	1.946(4)	Cu1–Cu4	5.2820(7)		

The three-dimensional structure is made up of the alternation of cationic and anionic layers that interact electrostatically and stack along the *c* direction (Figure 4 left). The anionic layers contain the $[\text{Cu}_7(\text{Hmesox})_6\text{Cl}_2]^{6-}$ heptanuclear clusters, whereas the $[\text{Ru}(\text{bpy})_3]^{2+}$ cations and Cl^- anions give rise to $\{[\text{Ru}(\text{bpy})_3]_2\text{Cl}\}_n^{3n+}$ cationic layers.

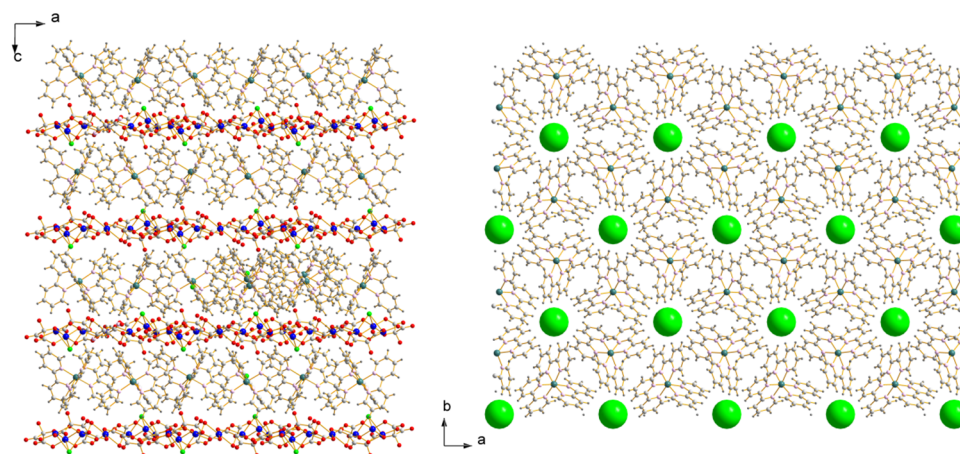


Figure 4. (left) View of the anionic layers containing the heptanuclear $[\text{Cu}_7(\text{Hmesox})_6\text{Cl}_2]^{6-}$ units alternating along the *c* direction with cationic layers containing $\{[\text{Ru}(\text{bpy})_3]_2\text{Cl}\}_n^{3n+}$ units in compound 2 (right). Arrangement of the chloride (space-filling green spheres) and $[\text{Ru}(\text{bpy})_3]^{2+}$ ions in the cationic $\{[\text{Ru}(\text{bpy})_3]_2\text{Cl}\}_n^{3n+}$ layers. (Same colour code as in Figure 3).

In the cationic $\{[\text{Ru}(\text{bpy})_3]_2\text{Cl}\}_n^{3n+}$ layers, each chloride ion is surrounded by six $[\text{Ru}(\text{bpy})_3]^{2+}$ cations which exist in both enantiomeric forms, Λ and Δ , related by an inversion centre, resulting in a nonchiral structure (Figure 4 right). The $[\text{Ru}(\text{bpy})_3]^{2+}$ cations display bonding distances and angles in the range of previously reported compounds [25,26]. The three-dimensional structure is stabilized by CH_3CN and H_2O crystallization solvent molecules.

3.2. Magnetic Properties of Compounds 1 and 2

The thermal variation of the product of the molar magnetic susceptibility per Cu_7 cluster times the temperature ($\chi_m T$) for compound 1 shows a room-temperature value of $2.15 \text{ cm}^3 \text{ K mol}^{-1}$ (Figure 5), which is appreciably lower than that expected value for seven non-interacting Cu^{II} ions ($2.8 \text{ cm}^3 \text{ K mol}^{-1}$ for $g = 2.1$) [27]. The $\chi_m T$ values continuously decrease on cooling the sample and reach a plateau at around $1.14 \text{ cm}^3 \text{ K mol}^{-1}$ between

70 and 20 K and a progressive decrease below 20 K (Figure 5). The low value at room-temperature and the shape of the plot denote a dominant moderate-strong antiferromagnetic interaction among the copper(II) ions through the alkoxide and carboxylate bridges.

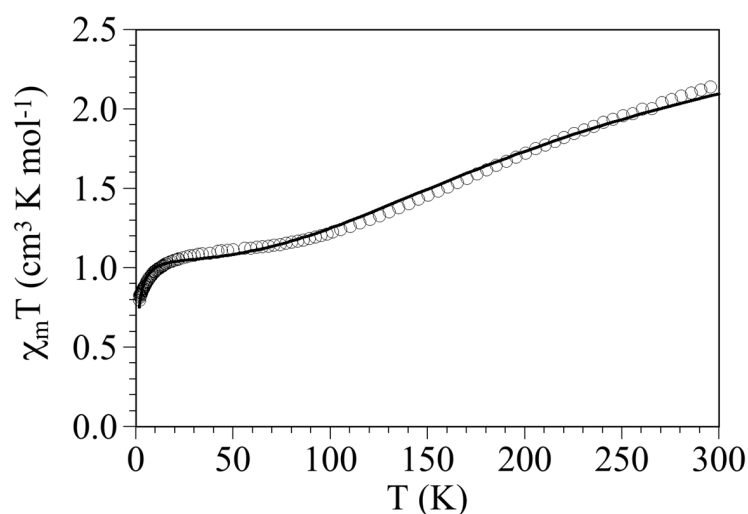
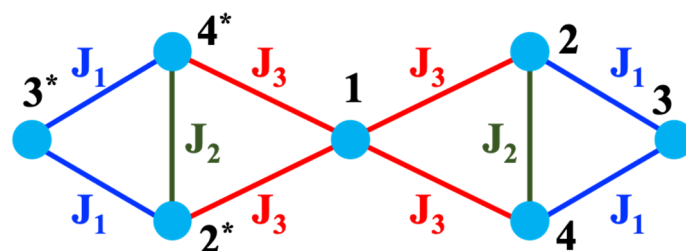


Figure 5. Temperature dependence of $\chi_m T$ for **1**. The solid line corresponds to the best fit to the model (see text).

In order to analyse the different exchange interactions existing in **1**, we can divide the plot into three regions attending to the different slopes observed. In the high-temperature region, with a fast decay of the $\chi_m T$ values, a strong antiferromagnetic coupling is operative, which more likely corresponds to antiferromagnetic interactions among the copper(II) ions of the trinuclear units through the mesoxalate–alkoxido linkers. This region concludes with two triangles, each with a $S = \frac{1}{2}$ spin ground state, yet which do not interact strongly with the central copper(II) ion (also $S = \frac{1}{2}$), leading to a plateau with a $\chi_m T$ value of around $1.14 \text{ cm}^3 \text{ K mol}^{-1}$, which is the value expected for three non-interacting $S = \frac{1}{2}$ ions. These three ions interact at very low temperatures through the carboxylate group and produce the additional progressive decrease in the $\chi_m T$ values. If we look in detail at the structure of compound **1**, we can distinguish three different coupling pathways (Scheme 2): two of them couple the Cu^{II} ions through alkoxide bridges and one through carboxylate ones. The magnetic-exchange coupling constants J_1 and J_2 correspond to the coupling through the alkoxide bridges, while J_3 corresponds to the interaction through the carboxylate bridges.



Scheme 2. Magnetic coupling scheme in compound **1**. Magnetic coupling through alkoxide bridges is shown in blue and green (J_1 and J_2), that through carboxylate bridges is shown in red (J_3). Symmetry code: (*) $1 - x, 1 - y, -z$.

The copper(II) ions in an octahedral or square pyramidal environment have their unpaired electron mainly in the $d_{x^2-y^2}$ orbital; thus, the carboxylate and the alkoxido oxygens filling the basal positions of the square pyramidal environment function as mediators of the magnetic coupling in these compounds. In order to simplify the number of adjustable parameters, we assume $J_{23} = J_{34} = J_1$, since both bridges have very similar Cu–O–Cu structural

parameters ($\text{Cu4-O15-Cu3} = 119.218(1)^\circ$ and $\text{Cu2-O9-Cu3} = 118.779(1)^\circ$) but different from those of the third bridge in the triangle ($\text{Cu4-O4-Cu2} = 139.387(2)^\circ$), for which J_2 is defined. On the other hand, we observe that the two exchange pathways connecting Cu1 with Cu2 and Cu4 through *anti-anti* carboxylate bridges are very similar and assume that they are equivalent. Of course, given the centro-symmetry of the Cu_7 cluster, we can write the following: $J_{12} = J_{14} = J_{12^*} = J_{14^*} = J_3$. Based on this magnetic exchange scheme, the phenomenological Hamiltonian can be written as follows (Scheme 2):

$$H_1 = -J_1 (S_2S_3 + S_3S_4 + S_2^*S_3^* + S_3^*S_4^*) - J_2 (S_2S_4 + S_2^*S_4^*) - J_3 (S_1S_2 + S_1S_4 + S_1S_2^* + S_1S_4^*)$$

The magnetic susceptibility data were analysed with PHI software (version 3.1.5) [28], and a good fit was obtained with the following parameters: $g = 2.225(2)$, $J_1 = 120.5(3) \text{ cm}^{-1}$, $J_2 = -203.1(5) \text{ cm}^{-1}$, $J_3 = -86.0(4) \text{ cm}^{-1}$ and $zj = -0.18(2) \text{ cm}^{-1}$ (the solid line in Figure 5 represents zj , the intercluster interaction, modeled using the mean field approximation). The values obtained indicate the occurrence of antiferromagnetic interactions through the alkoxido and carboxylate bridges, confirming the starting hypothesis.

Previous studies conducted by our research group showed that the most important parameter in the interaction between Cu(II) ions through the alkoxide bridge of the mesoxalate ligand is the Cu–O–Cu bond angle. For angles below 114° , a ferromagnetic interaction can occur, whereas for angles above 114° , the interaction becomes antiferromagnetic. Moreover, the strength of the antiferromagnetic interaction increases as the Cu–O–Cu angle increases (Figure 6) [23].

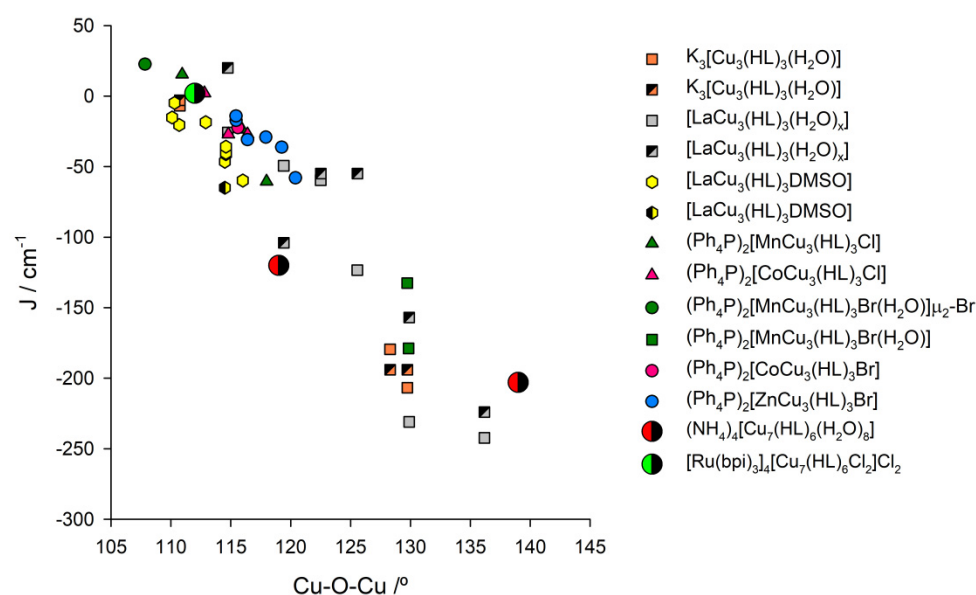
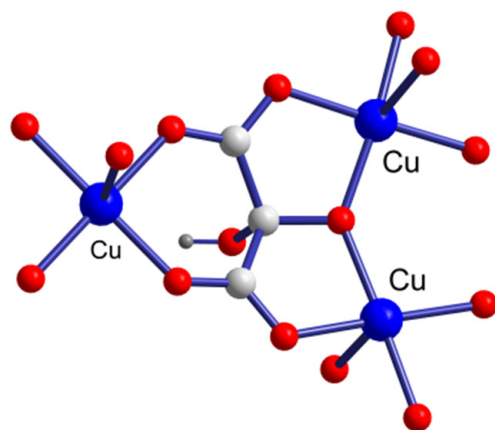


Figure 6. Dependence of the magnetic coupling constant, J , with the Cu–O–Cu bond angle in copper(II) mesoxalate compounds. Solid symbols partially filled in black correspond to experimental values, while the remaining symbols correspond to calculated values. Compounds **1** and **2** are shown with bigger size symbols to enhance their visibility. H_4L = mesoxalic acid.

In compound **1**, we find a moderate antiferromagnetic coupling between Cu2 and Cu3 and between Cu3 and Cu4, with bridging Cu–O–Cu angles around 119° ($J_1 = -120.5(3) \text{ cm}^{-1}$). As expected, a stronger antiferromagnetic interaction occurs between Cu2 and Cu4, with a Cu–O–Cu bridging angle of $139.387(2)^\circ$ ($J_2 = -203.1(5) \text{ cm}^{-1}$). Therefore, the values found in **1** show the expected trend and are within the expected range observed in previous studies [23]. Additionally, as observed experimentally, J_3 ($-86.0(4) \text{ cm}^{-1}$) is also expected to be antiferromagnetic since it corresponds to the coupling of two Cu^{II} ions via a single *anti-anti* carboxylate bridge (Scheme 3) [1,29–31]. However, this magnetic coupling constant is more difficult to compare because most studies were conducted with oxalate ligands

connecting two Cu^{II} ions through a double *anti-anti* carboxylate bridge [2,32,33]. Furthermore, the bridging mode of the μ_3 -mesoxalate in compound **1** is unique, since it couples antiferromagnetically two copper(II) ions via an alkoxide bridge, and these two atoms are, at the same time, antiferromagnetically coupled with a third copper(II) via two single *anti-anti* carboxylate groups, leading to a situation that may exhibit spin frustration [34,35].



Scheme 3. μ_3 -bridging mode of the Hmesoxalate ligand in compound **1**.

The thermal dependence of the $\chi_m T$ product for compound **2** per Cu₇ cluster shows, at room temperature, a value of $2.6 \text{ cm}^3 \text{ K mol}^{-1}$ (Figure 7). This value is somewhat lower than the expected one for seven isolated spin doublets ($2.8 \text{ cm}^3 \text{ K mol}^{-1}$ for $g = 2.1$). When the sample is cooled, $\chi_m T$ decreases to reach a minimum value of $2.4 \text{ cm}^3 \text{ K mol}^{-1}$ at around 100 K. Below this temperature, $\chi_m T$ increases to reach a maximum value of $3.0 \text{ cm}^3 \text{ K mol}^{-1}$ at 22 K, followed by a sharp decrease below this temperature (Figure 7). This behaviour is indicative of the occurrence of both antiferromagnetic and ferromagnetic interactions in the heptanuclear unit.

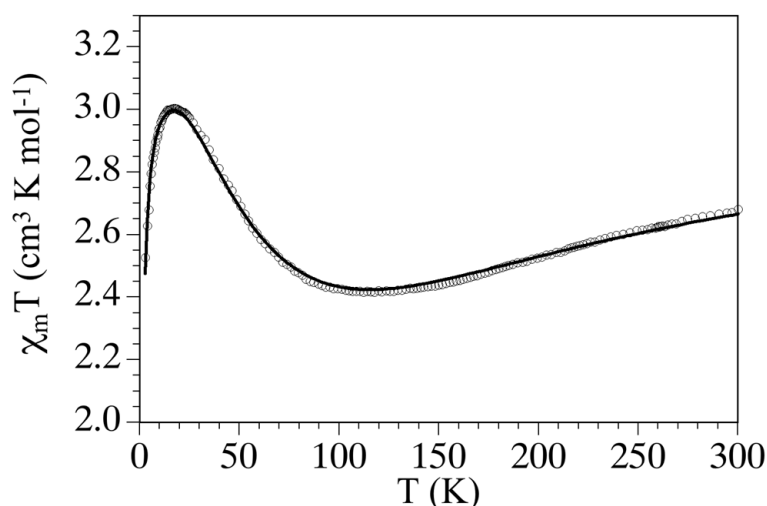
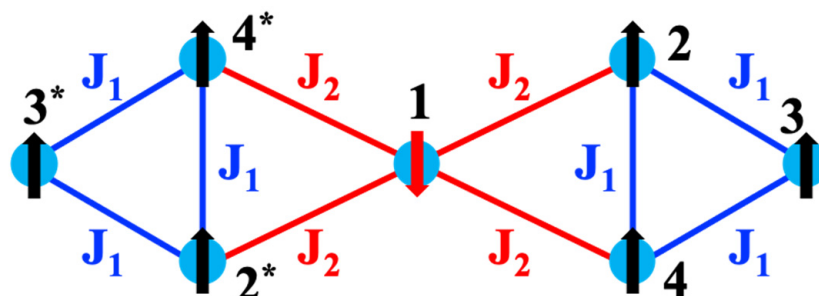


Figure 7. Temperature dependence of $\chi_m T$ for **2**. The solid line corresponds to the best fit to the model (see text).

Here again, we have a very complex molecule with seven spin carriers and many magnetic exchange pathways. In order to avoid the over parametrization of the model, looking at the symmetry and at the nature of the bridging groups, we tried to simplify the system. In previous studies, we found that a ferromagnetic coupling can be found in copper(II)/mesoxalate trinuclear units with Cu–O–Cu bridging angles lower than 114° [23]. Since the three Cu–O–Cu bond angles are similar along the three sides of the triangle

(Cu3–O15–Cu4 = 112.34(2)°, Cu4–O4–Cu2 = 111.39(18)° and Cu2–O9–Cu3 = 113.18(19)°, Table 4), we use the same coupling constant for the three pathways (J_1 in Scheme 4). As we did in compound **1**, we assume that the coupling between the central Cu1 centre and Cu2 and Cu4 are also antiferromagnetic since they correspond to the *anti-anti* carboxylate bridges (J_2 in Scheme 4).



Scheme 4. Magnetic coupling scheme in compound **2**. The magnetic coupling through alkoxide and carboxylate bridges are shown in blue (J_1) and red (J_2), respectively. Symmetry code: (*) $1 - x, 1 - y, -z$.

Using this exchange scheme, the phenomenological Hamiltonian used to fit the magnetic data can be written as follows:

$$H_2 = -J_1 (S_2S_3 + S_3S_4 + S_2S_4 + S_2^*S_3^* + S_3^*S_4^* + S_2^*S_4^*) - J_2 (S_1S_2 + S_1S_4 + S_1S_2^* + S_1S_4^*)$$

The magnetic susceptibility data were fitted with the PHI software (version 3.1.5) [28], and a very good fit was obtained in the whole temperature range with the following parameters: $g = 2.1688(3)$, $J_1 = 1.96(4) \text{ cm}^{-1}$, $J_2 = -114.9(2) \text{ cm}^{-1}$ and $zj = -0.129(1) \text{ cm}^{-1}$ (solid line in Figure 7). On one hand, in contrast to compound **1**, we find a ferromagnetic coupling within both mesoxalate–alkoxido-bridged Cu2–Cu3–Cu4 triangles. On the other side, as observed in compound **1**, the central Cu1 is antiferromagnetically coupled with the Cu2 and Cu4 centres of the triangles. This behaviour agrees with the presence of similar *anti-anti* carboxylate bridges connecting the copper(II) centres, as in **1**. The value obtained for J_1 is weak and ferromagnetic, in agreement with our previous results, showing that for Cu–O–Cu bond angles below 114°, the coupling is ferromagnetic (see above). In compound **2**, these angles are Cu3–O15–Cu4 = 112.34(2)°, Cu4–O4–Cu2 = 111.39(18)° and Cu2–O9–Cu3 = 113.18(19)°; therefore, a weak ferromagnetic coupling is expected, in agreement with the experimental result ($J_1 = 1.96(4) \text{ cm}^{-1}$). On the other hand, the coupling through the two single *anti-anti* carboxylate bridges for this compound is somewhat stronger to that found in **1**. This behaviour can be understood considering the shorter Cu1–Cu2 and Cu1–Cu4 distances compared to those found in **1** (Tables 2 and 4).

The ferromagnetic J_1 and antiferromagnetic J_2 coupling constants lead to a spin distribution, as shown in Scheme 4, where the six spins on the copper(II) triangles are aligned in a parallel way to each other and antiparallel to the central Cu1 spin, leading to a $S = 5/2$ spin ground state. Accordingly, the isothermal magnetizations at 2 and 5 K show saturation values very close to $5.0 \mu_B$, which is the expected value for a $S = 5/2$ ground spin state (Figure 8). Furthermore, they can be satisfactorily reproduced with a Brillouin function for an $S = 5/2$ ground spin state (solid lines in Figure 8) with g values close to 2.

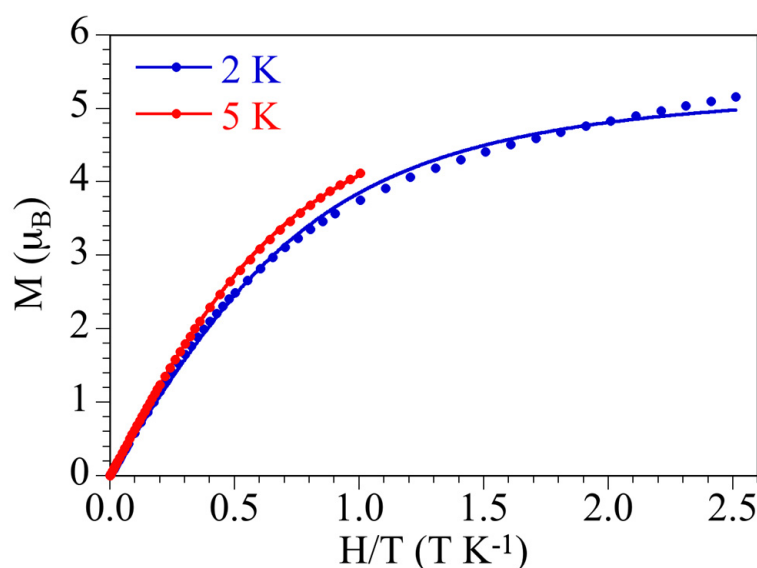


Figure 8. Isothermal magnetization of compound **2** at 2 and 5 K. The solid lines are the best fit to the Brillouin function for an $S = 5/2$ ground spin state.

3.3. Spectroscopic Measurements

The excitation spectrum of a solid-state sample of compound **2**, monitored at 600 nm, shows two prominent bands around 325 and 480 nm (Figure 9). These bands can be assigned to charge-transfer $d \rightarrow \pi^*$ transitions, similar to those observed in $[\text{Ru}(\text{bpy})_3]\text{Cl}_2$ [36]. Moreover, when the compound is excited at 480 nm, an intense emission band is detected around 600 nm. These results are similar to those found in the $[\text{Ru}(\text{bpy})_3]\text{Cl}_2$ [36], showing an emission band at 600 nm with a lifetime around 0.7–0.9 μs at room temperature. This emission band is associated with a triplet–singlet transition, but with a short lifetime because the selection rules are partially removed.

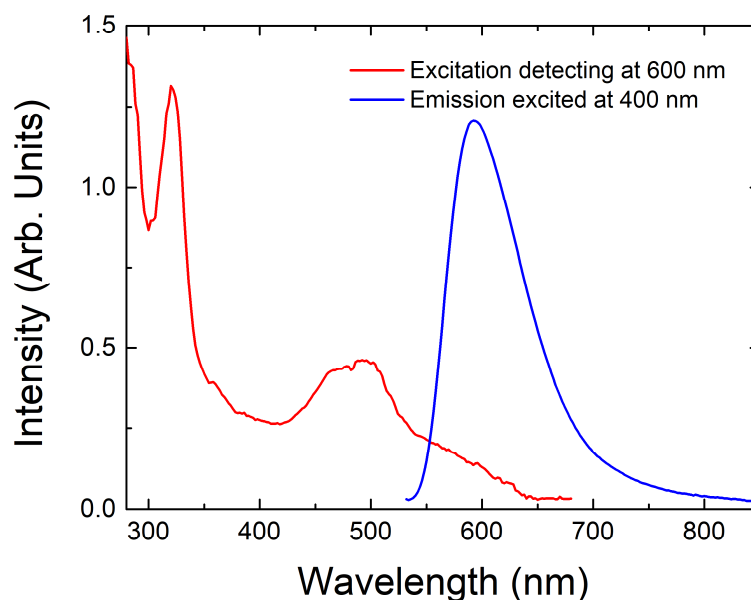


Figure 9. Emission and excitation spectra of compound **2** obtained, respectively, under excitation at 480 nm and detection at 600 nm.

4. Conclusions

We prepared two new compounds: $(\text{NH}_4)_4[\text{Cu}_7(\text{Hmesox})_6(\text{H}_2\text{O})_8] \cdot 10\text{H}_2\text{O}$ (**1**) and $[\text{Ru}(\text{bpy})_3]_4[\text{Cu}_7(\text{Hmesox})_6\text{Cl}_2]\text{Cl}_2 \cdot 2\text{CH}_3\text{CN} \cdot 12\text{H}_2\text{O}$ (**2**) containing very similar centro-

symmetric heptanuclear mesoxalate-bridged copper(II) clusters formed by two Cu₃ triangles connected to a central Cu atom. The structural analysis of both heptanuclear Cu^{II} clusters show that the copper(II) ions in the triangles are connected via alkoxido bridges, whereas the central Cu atom is connected to two of the three Cu centres of each triangle via *anti-anti* carboxylate bridges. In compound **1**, the structural parameters indicate the presence of two different coupling constants inside the triangle (J_1 and J_2), whereas in compound **2**, both constants are the same (J_1). The magnetic properties show that in compound **1**, J_1 and J_2 are antiferromagnetic, in agreement with the Cu–O–Cu bond angles, leading to a spin frustration inside the triangle. In contrast, in compound **2**, J_1 is weak and ferromagnetic. In both compounds, the coupling through the anti-anti carboxylate bridges between the central Cu centre and the triangles (J_3 in **1** and J_2 in **2**) are moderate and antiferromagnetic, as expected given the presence of *anti-anti* carboxylate bridges. The use of these $3J$ and $2J$ models for compounds **1** and **2**, respectively, allows us to reproduce, in a very satisfactory way, the magnetic data of both compounds. In all cases, the J values found agree with previous magneto-structural correlations. Comparing **1** and **2**, we observe that small differences in the Cu–O–Cu bridging angles are responsible for the different magnetic behaviour. Finally, the anionic character of these heptanuclear clusters allows the incorporation of counterions that can introduce other properties in addition to the magnetic ones. Thus, compound **2** contains a luminescent [Ru(bpy)₃]²⁺ counterion that displays its characteristic luminescent properties.

Supplementary Materials: The following supporting information can be downloaded at: <https://www.mdpi.com/article/10.3390/magnetochemistry10120093/s1>, Figure S1: Powder X-Ray Diffraction pattern of compound **1** compared to the pattern simulated from the single crystal structure; Figure S2: Powder X-Ray Diffraction pattern of compound **2** compared to the pattern simulated from the single crystal structure.

Author Contributions: Conceptualization, B.G.-H. and J.S.; methodology, B.G.-H. and J.S.; validation, B.G.-H. and J.S.; investigation, B.G.-H., S.M., I.G., J.S. and C.J.G.-G.; data curation, I.G., S.M., B.G.-H. and C.J.G.-G.; writing—original draft preparation, J.S., C.J.G.-G. and B.G.-H.; writing—review and editing, B.G.-H., J.S., C.J.G.-G. and C.J.; funding acquisition, C.J.G.-G. and C.J. All authors have read and agreed to the published version of the manuscript.

Funding: C. J. G. G. acknowledges the support of the Advanced Materials program, supported by the Spanish MCIN with funding from the European Union NextGeneration EU (PRTR-C17.I1) and the Generalitat Valenciana (project MFA-2022-057). We also acknowledge the Grant PID2021-125907NB-I00, funded by MCIN/AEI/10.13039/501100011033 and by “ERDF A way of making Europe”, as well as project CIPROM-2022-060 from the Generalitat Valenciana, for financial support.

Data Availability Statement: The data will be provided upon request to the corresponding author.

Acknowledgments: JS and BGH thank the Departamento de Química de la Universidad de La Laguna for financial support and SEGAI-ULL for X-ray measurements.

Conflicts of Interest: The authors declare no conflicts of interest.

Appendix A

CCDC 1909005 and 1909004 contain the supplementary crystallographic data for compounds **1** and **2**, respectively. These data can be obtained free of charge via <http://www.ccdc.cam.ac.uk/conts/retrieving.html> or from Cambridge Crystallographic Data Centre, 12 Union Road, Cambridge CB2 1EZ, UK; fax: (+44) 1223-336-033; or e-mail: deposit@ccdc.cam.ac.uk.

References

1. Julve, M.; Verdaguer, M.; Kahn, O.; Gleizes, A.; Philoche-Levisalles, M. Tunable exchange interaction in μ -oxalato copper(II) dinuclear complexes. *Inorg. Chem.* **1983**, *22*, 368–370. [[CrossRef](#)]
2. Julve, M.; Gleizes, A.; Chamoreau, L.M.; Ruiz, E.; Verdaguer, M. Antiferromagnetic Interactions in Copper(II) μ -Oxalato Dinuclear Complexes: The Role of the Counterion. *Eur. J. Inorg. Chem.* **2017**, *2018*, 509–516. [[CrossRef](#)]

3. Julve, M.; Faus, J.; Verdaguer, M.; Gleizes, A. Copper(II), a chemical Janus: Two different (oxalato)(bipyridyl)copper(II) complexes in one single crystal. Structure and magnetic properties. *J. Am. Chem. Soc.* **2002**, *106*, 8306–8308. [[CrossRef](#)]
4. Castro, I.; Calatayud, M.L.; Orts-Arroyo, M.; Marino, N.; De Munno, G.; Lloret, F.; Ruiz-García, R.; Julve, M. Oxalato as polyatomic coordination center and magnetic coupler in copper(II)-polypyrazole inverse polynuclear complexes and coordination polymers. *Coord. Chem. Rev.* **2022**, *471*, 214730. [[CrossRef](#)]
5. Sletten, J.; Soerensen, A.; Julve, M.; Journaux, Y. A tetranuclear hydroxo-bridged copper(II) cluster of the cubane type. Preparation and structural and magnetic characterization of tetrakis [(2,2'-bipyridyl)hydroxocopper(II)] hexafluorophosphate. *Inorg. Chem.* **1990**, *29*, 5054–5058. [[CrossRef](#)]
6. Ruiz-Perez, C.; Sanchiz, J.; Molina, M.H.; Lloret, F.; Julve, M. Ferromagnetism in malonato-bridged copper(II) complexes. synthesis, crystal structures, and magnetic properties of $\{[\text{Cu}(\text{H}_2\text{O})_3][\text{Cu}(\text{mal})_2(\text{H}_2\text{O})]\}_n$ and $\{[\text{Cu}(\text{H}_2\text{O})_4]_2[\text{Cu}(\text{mal})_2(\text{H}_2\text{O})][\text{Cu}(\text{mal})_2(\text{H}_2\text{O})_2][\text{Cu}(\text{H}_2\text{O})_4][\text{Cu}(\text{mal})_2(\text{H}_2\text{O})_2]\}$ (H_2mal = malonic Acid). *Inorg. Chem.* **2000**, *39*, 1363–1370. [[CrossRef](#)]
7. Sanchiz, J.; Pasán, J.; Fabelo, O.; Lloret, F.; Julve, M.; Ruiz-Pérez, C. $[\text{Cu}_3(\text{Hmesox})_3]^{3-}$: A Precursor for the Rational Design of Chiral Molecule-Based Magnets (H_4mesox = 2-dihydroxymalonic acid). *Inorg. Chem.* **2010**, *49*, 7880–7889. [[CrossRef](#)]
8. Gil-Hernández, B.; Gili, P.; Sanchiz, J. A ferromagnetically coupled copper(II) trinuclear secondary building unit as precursor for the preparation of molecule-based magnets. *Inorg. Chim. Acta* **2011**, *371*, 47–52. [[CrossRef](#)]
9. Gil-Hernández, B.; Gili, P.; Vieth, J.K.; Janiak, C.; Sanchiz, J. Magnetic ordering in two molecule-based (10,3)-a nets prepared from a copper(II) trinuclear secondary building unit. *Inorg. Chem.* **2010**, *49*, 7478–7490. [[CrossRef](#)]
10. Gil-Hernández, B.; Savvin, S.; Makhlofi, G.; Núñez, P.; Janiak, C.; Sanchiz, J. Proton conduction and long-range ferrimagnetic ordering in two isostructural copper(II) mesoxalate metal-organic frameworks. *Inorg. Chem.* **2015**, *54*, 1597–1605. [[CrossRef](#)]
11. Mistry, S.; Sutter, J.P.; Natarajan, S. Stabilization of Cu_7 clusters in azide networks: Syntheses, structures and magnetic behaviour. *Dalton Trans.* **2016**, *45*, 5140–5150. [[CrossRef](#)]
12. Ferrer, S.; Aznar, E.; Lloret, F.; Castineiras, A.; Liu-Gonzalez, M.; Borrás, J. One-dimensional metal-organic framework with unprecedented heptanuclear copper units. *Inorg. Chem.* **2007**, *46*, 372–374. [[CrossRef](#)] [[PubMed](#)]
13. Bromhead, J.A.; Young, C.G. Tris(2,2'-Bipyridine)Ruthenium(II) Dichloride Hexahydrate. *Inorg. Synth.* **1982**, *21*, 127. [[CrossRef](#)]
14. Bain, G.A.; Berry, J.F. Diamagnetic Corrections and Pascal's Constants. *J. Chem. Educ.* **2008**, *85*, 532–536. [[CrossRef](#)]
15. Bruker AXS. APEX2; Bruker: Billerica, MA, USA, 2012.
16. Sheldrick, G.M. *Program SADABS: Area-Detector Absorption Correction*; University of Göttingen: Göttingen, Germany, 1996.
17. Sheldrick, G.M. Crystal structure refinement with SHELXL. *Acta Crystallogr. C Struct. Chem.* **2015**, *71*, 3–8. [[CrossRef](#)] [[PubMed](#)]
18. Hubschle, C.B.; Sheldrick, G.M.; Dittrich, B. ShelXle: A Qt graphical user interface for SHELXL. *J. Appl. Crystallogr.* **2011**, *44*, 1281–1284. [[CrossRef](#)]
19. Hooft, R.W.W. *Collect*; Nonius BV: Delft, The Netherlands, 1998.
20. Sheldrick, G.M. *SADABS, Program for Area Detector Adsorption Correction*; Institute for Inorganic Chemistry, University of Göttingen: Göttingen, Germany, 1996.
21. Sheldrick, G.M. *SHELXL-97, Program for the Refinement of Crystal Structure from Diffraction Data*; University of Göttingen: Göttingen, Germany, 1997.
22. Addison, A.W.; Rao, T.N.; Reedijk, J.; van Rijn, J.; Verschoor, G.C. Synthesis, structure, and spectroscopic properties of copper(II) compounds containing nitrogen–sulphur donor ligands; the crystal and molecular structure of aqua [1,7-bis(N-methylbenzimidazol-2'-yl)-2,6-dithiaheptane] copper(II) perchlorate. *J. Chem. Soc. Dalton Trans.* **1984**, 1349–1356. [[CrossRef](#)]
23. Gil-Hernández, B.; Calahorra, A.J.; Gili, P.; Sanchiz, J. Effect of the apical ligand on the geometry and magnetic properties of copper(II)/mesoxalate trinuclear units. *Dalton Trans.* **2017**, *46*, 5260–5268. [[CrossRef](#)]
24. Gil-Hernández, B.; Gili, P.; Pasán, J.; Sanchiz, J.; Ruiz-Pérez, C. Two-dimensional (6,3) networks obtained with the $\{\text{Cu}_3(\text{Hmesox})_3\}^{3-}$ secondary building unit (H_4mesox = mesoxalic acid). *CrystEngComm* **2012**, *14*, 4289–4297. [[CrossRef](#)]
25. Harrowfield, J.M.; Sobolev, A.N. The Crystal Structure of Tris(2,2'-bipyridine)ruthenium(II) Perchlorate. *Aust. J. Chem.* **1994**, *47*, 763. [[CrossRef](#)]
26. Rillema, D.P.; Jones, D.S. Structure of tris(2,2'-bipyridyl)ruthenium(II) hexafluorophosphate, $[\text{Ru}(\text{bipy})_3][\text{PF}_6]_2$; X-ray crystallographic determination. *J. Chem. Soc. Chem. Commun.* **1979**, 849–851. [[CrossRef](#)]
27. Kahn, O. *Molecular Magnetism*; VCH: New York, NY, USA, 1993.
28. Chilton, N.F.; Anderson, R.P.; Turner, L.D.; Soncini, A.; Murray, K.S. PHI: A powerful new program for the analysis of anisotropic monomeric and exchange-coupled polynuclear d- and f-block complexes. *J. Comput. Chem.* **2013**, *34*, 1164–1175. [[CrossRef](#)] [[PubMed](#)]
29. Pasán, J.; Delgado, F.S.; Rodríguez-Martín, Y.; Hernández-Molina, M.; Ruiz-Pérez, C.; Sanchiz, J.; Lloret, F.; Julve, M. Malonate-based copper(II) coordination compounds: Ferromagnetic coupling controlled by dicarboxylates. *Polyhedron* **2003**, *22*, 2143–2153. [[CrossRef](#)]
30. Rodríguez-Martín, Y.; Hernández-Molina, M.; Delgado, F.S.; Pasán, J.; Ruiz-Pérez, C.; Sanchiz, J.; Lloret, F.; Julve, M. Structural versatility of the malonate ligand as a tool for crystal engineering in the design of molecular magnets. *CrystEngComm* **2002**, *4*, 522–535. [[CrossRef](#)]
31. Delgado, F.S.; Ruiz-Pérez, C.; Sanchiz, J.; Lloret, F.; Julve, M. Versatile supramolecular self-assembly Part II. Network formation and magnetic behaviour of copper(II) malonate anions in ammonium derivatives. *CrystEngComm* **2006**, *8*, 530–544. [[CrossRef](#)]

32. Julve, M.; Verdaguer, M.; Gleizes, A.; Philoche-Levisalles, M.; Kahn, O. Design of μ -oxalato copper(II) binuclear complexes exhibiting expected magnetic properties. *Inorg. Chem.* **1984**, *23*, 3808–3818. [[CrossRef](#)]
33. Calatayud, M.L.; Orts-Arroyo, M.; Julve, M.; Lloret, F.; Marino, N.; De Munno, G.; Ruiz-García, R.; Castro, I. Magneto-structural correlations in asymmetric oxalato-bridged dicopper(II) complexes with polymethyl-substituted pyrazole ligands. *J. Coord. Chem.* **2018**, *71*, 657–674. [[CrossRef](#)]
34. Ferrer, S.; Lloret, F.; Bertomeu, I.; Alzuet, G.; Borrás, J.; García-Granda, S.; Liu-González, M.; Haasnoot, J.G. Cyclic Trinuclear and Chain of Cyclic Trinuclear Copper(II) Complexes Containing a Pyramidal $\text{Cu}_3\text{O}(\text{H})$ Core. Crystal Structures and Magnetic Properties of $[\text{Cu}_3(\mu_3\text{-OH})(\text{aaat})_3(\text{H}_2\text{O})_3](\text{NO}_3)_2 \cdot \text{H}_2\text{O}$ [aaat = 3-Acetylamino-5-amino-1,2,4-triazolate] and $\{[\text{Cu}_3(\mu_3\text{-OH})(\text{aat})_3(\mu_3\text{-SO}_4)] \cdot 6\text{H}_2\text{O}\}_n$ [aat = 3-Acetylamino-1,2,4-triazolate]: New Cases of Spin-Frustrated Systems. *Inorg. Chem.* **2002**, *41*, 5821–5830. [[CrossRef](#)]
35. Ferrer, S.; Lloret, F.; Pardo, E.; Clemente-Juan, J.M.; Liu-Gonzalez, M.; Garcia-Granda, S. Antisymmetric exchange in triangular tricopper(II) complexes: Correlation among structural, magnetic, and electron paramagnetic resonance parameters. *Inorg. Chem.* **2012**, *51*, 985–1001. [[CrossRef](#)]
36. Lytle, F.E.; Hercules, D.M. Luminescence of tris (2, 2'-bipyridine) ruthenium (II) dichloride. *J. Am. Chem. Soc.* **1969**, *91*, 253–257. [[CrossRef](#)]

Disclaimer/Publisher's Note: The statements, opinions and data contained in all publications are solely those of the individual author(s) and contributor(s) and not of MDPI and/or the editor(s). MDPI and/or the editor(s) disclaim responsibility for any injury to people or property resulting from any ideas, methods, instructions or products referred to in the content.